

## Computational study of the PCM charging in the latent heat thermal energy storage system

Hayder A. Al-Salami<sup>\*</sup>, Nabeel S. Dhaidan<sup>\*\*</sup>, Fadhel N. Al-Mousawi<sup>\*\*\*</sup>

<sup>\*</sup> Department of Mechanical Engineering, College of Engineering, University of Kerbala  
E-mail:- [e.hayder81@gmail.com](mailto:e.hayder81@gmail.com)

<sup>\*\*</sup> Department of Mechanical Engineering, College of Engineering, University of Kerbala  
E-mail:- [nabeel.sh@uokerbala.edu.iq](mailto:nabeel.sh@uokerbala.edu.iq)

<sup>\*\*\*</sup> Department of Mechanical Engineering, College of Engineering, University of Kerbala  
E-mail:- [fadhelnor@gmail.com](mailto:fadhelnor@gmail.com)

Received: 14 February 2024; Revised: 11 March 2024; Accepted: 28 March 2024

### Abstract

This paper presents the computational investigation of the charging characteristics of PCM inside a latent heat thermal energy storage (LHTES) unit that consists of a horizontal heat exchanger type of the inner tube and outer shell using ANSYS/FLUENT software. The melting process numerically tested for the heat transfer fluid HTF (water) inlet temperature (60, 70, and 80 °C), and the PCM's initial temperature is 15 °C. Also, this study examined the effect of the mushy zone constant. Extensive measures show that charging time decreases with increased water inlet temperature. The melting of PCM completes in a time of 260 minutes when using a water inlet temperature of 60 °C, while the melting time reaches 182 minutes when the water inlet temperature is 70 °C, and the melting completes in a time of 145 minutes by using the hot water entry temperature of 80 °C. When the water inlet temperature increased from 60 °C to 70 °C and 80 °C, respectively, the melting time was saved by about 30% and 44%. The best melting time reduction is achieved at an HTF inlet temperature of 80 °C. In addition, the melting time increased as constant values rose in the mushy zone. The melting times are 182, 191, and 200 minutes for mushy zone constants  $10^5$ ,  $10^6$ , and  $10^7$ , respectively. So, the mushy zone constant of 105 leads to the best reduction in melting time.

**Keywords:** PCM, Charging, LHTES, Natural convection, Mushy zone constant, Melting time.

## 1. Introduction

Fossil fuels such as oil, natural gas, and coal have been the primary energy sources for many years. As a result of the increase in population and the accompanying increase in the consumption of energy resources in manufacturing, operating factories, means of transportation, heating homes, and producing electricity, and due to the increased intensity of competition between countries of the world, especially the major industrial countries in the field of manufacturing and factories, all of this has led to a rise in global demand for oil, natural gas, and coal. As a result of the changes occurring in the climate due to pollution from carbon emissions associated with high energy consumption, as well as the global energy crisis due to the depletion of traditional energy sources, it has become necessary to reduce energy consumption and rely on environmentally friendly renewable energy sources. Renewable energy sources are not always available when needed. The time difference between energy sources and demand is a significant challenge. The solution to this problem is using the energy storage systems of one of its types (thermal, chemical, electrical, kinetic, etc.) to continuously provide energy at the time of its interruption from its prepared source.

Phase change materials (PCM) are a promising thermal storage medium. Thermal energy storage systems depend on phase change materials (PCMs), which store sensible and latent energies [1]. Latent thermal energy storage systems have recently been widely used in various fields.

Tabular thermal energy storage devices consist of an inner tube that transports the heat transfer fluid, which serves as a source of thermal energy causing the melting of the PCM, an insulated outer shell, and PCM that fills the space between the inner tube and the outer shell. The process of melting PCM is affected by several factors, including the heat transfer fluid (HTF) inlet temperature, the mushy zone constant, the mesh size, the time-step, and other factors.

Dutta et al. [2] performed a numerical and experimental investigation on the performance of the latent heat storage system during the PCM melting processes. Paraffin wax was used as a PCM material, and the water was used as an HTF. Another researcher, Ezan et al. [3], experimentally studied ice's charging and discharging process as a PCM inside a horizontal shell and tube LHTES device under the impact of some parameters. The natural convection controlled the melting process in the upper section, and the inlet temperature of the heat transfer fluid and the amount of flow affected the melting time. Adine and El Qarnia [4] numerically studied the thermal performance of two PCMs melting in the tabular heat exchanger. They studied the effect of a set of parameters: the HTF entrance temperature, its mass

flow rate, and the length of the storage unit on the melting process. Darzi et al. [5] achieved numerical research on the properties of melting PCM in horizontal annular storage units with concentric and eccentric arrays of inner tubes. Using the eccentric case, they studied the effect of increasing the convection area on the melting rate.

Hosseini et al. [6] numerically and experimentally examined the impact of buoyancy-driven convection on the PCM thawing within a horizontal thermal storage unit. They also examined the effect of the HTF entrance temperature on the melting time. Longeon et al. [7] performed a numerical and experimental study to inspect the influence of the heat transfer mechanism and injection side on the melting and solidification of paraffin RT35 inside the vertical thermal storage system. They investigated the impacts of free convection and the HTF flow direction on the melting process. Wang et al. [8] numerically studied the impact of the HTF's flow rate and inlet temperatures on the PCM melting process placed inside a horizontal LHTES unit. Avci and Yazici [9] presented an experimental study of the thermal properties of a PCM material placed inside a horizontal annular cavity of the LHTES system. The PCM melted due to natural convection, where the molten material rose to the top due to its melting, leading to the melting of the rest of the solid material.

Agrawal and Sarviya [10] computationally researched the paraffin wax melting in a horizontal tabular LHTES unit. The constant temperature principle was used for the inner tube, and a two-dimensional numerical model was used to investigate the thermal behaviour of PCM. Alshara [11] studied numerically PCM melting in concentric horizontal LHTES whose outer shell is insulated and uses water as the heat transfer fluid. He also studied the influence of the water inlet temperature on the PCM charging duration. Dukhan et al. [12] presented an experimental study about charging RT42 PCM inside an LHTES device. Water was used as an HTF, and the device was a concentric shell-and-tube type. The impact of the HTF's inlet temperature on reducing the charging time was studied. Seddegh et al. [13] presented experimentally and numerically the mechanism of heat transfer of PCM put in a vertical (LHTES) unit. They studied the impact of natural convection on this heat transfer. Ali et al. [14] conducted experiments to explore the thermal behaviour of PCM charged inside the LHTES device using water as an HTF. The temperature variation between the external shell and inner pipe with different mass flow rates was experimentally calculated.

In this study, computational fluid dynamics (CFD) modelling on the melting of phase change material (PCM) in an (LHTES) unit was performed. The effect of HTF (water) inlet temperature and the mushy zone constant on the melting of PCM are investigated numerically.

## 2. Physical Model

Fig. (1) describes the physical domain that involves (PCM) placed inside the annular cylinder of a horizontally oriented heat exchanger. The PCM heat exchanger consists of double-concentric pipes. The outer pipe (shell) with radius ( $r_o$ ) that is thermally insulated is composed of acrylic material and has a diameter of 75 mm and a wall thickness of 2.5 mm. The inner pipe is made of copper with a radius ( $r_i$ ) and has a diameter of 25 mm with a wall thickness of 0.9 mm. The heat exchanger measures 500 mm in length. The PCM (RT-42 Rubitherm) fills the annular space between two pipes with a melting range of 38 to 42 °C. The melt of PCM was assumed to be homogenous, laminar, incompressible and Newtonian fluid. Table (1) lists the thermophysical characteristics of the employed PCMs. The storage cell's heat source is a hot water HTF that flows through the inner pipe. The melting procedure in an annular chamber is a two-dimensional matter. It is necessary to define melting inside the horizontal annular heat exchanger in the radial and angular coordinates ( $r, \theta$ ).  $T_{ini}$  represents the initial temperature of the PCM when it is in the solid state and equal to 15 °C. The heat transfer fluid enters the system at a temperature of  $T_w$  and a constant velocity of  $U_{in}$  and exists at atmospheric pressure. All walls are designed to be non-slip.

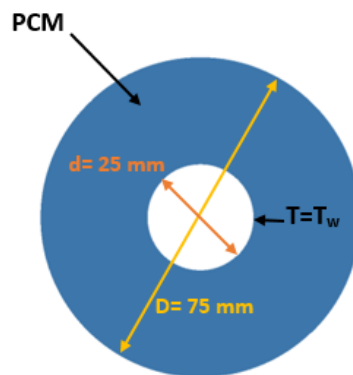


**Figure 1. Physical model of the problem.**

**Table 1. Physical and thermal properties of the PCM.**

Solidus Temperature, $T_s$	38 °C
Liquidus Temperature, $T_l$	42 °C
Melting latent heat of, $\Delta H$	174 kJ.kg <sup>-1</sup>
Density, $\rho$	880 kg/m <sup>3</sup> (solid) 760 kg/m <sup>3</sup> (liquid)
Dynamic viscosity, $\mu$	0.02728 kg/m.s
Coefficient of thermal expansion, $\beta$	0.0008 1/k
Specific heat capacity, $C_p$	2 kJ/kg k
Thermal conductivity, $k$	0.2 W/m <sup>2</sup> °k

### 3. The Governing Equations

In order to analyze PCM melting in a concentric annular cell, the following continuity, momentum, and energy equations are used:

$$\frac{\partial \rho}{\partial t} + \nabla \cdot (\rho V) = 0 \quad (1)$$

$$\frac{\partial(\rho V)}{\partial t} + \nabla \cdot (\rho VV) = \mu \nabla^2 V - \nabla P + S_u \quad (2)$$

$$\frac{\partial}{\partial t} (\rho H) + \nabla \cdot (\rho VH) = \nabla \cdot (K \nabla T) \quad (3)$$

Where  $\rho$ ,  $\mu$ , and  $k$  represent the density, viscosity, and thermal conductivity of phase change material (PCM), respectively.

The body force component in the momentum equation may be approximated using the Boussinesq approximation, which relies on a reference density ( $\rho_{ref}$ ), temperature ( $T_{ref}$ ), and thermal expansion coefficient ( $\beta$ ).

$$\text{Where} \quad S_u = S_D + S_g \quad (3a)$$

$$\text{And} \quad S_g = \rho_{ref} g \beta (T - T_{ref}) \quad (3b)$$

Also 
$$\beta = -\frac{1}{\rho} \left( \frac{\partial \rho}{\partial T} \right) P \quad (3c)$$

Where  $S_g$  represents the body force of buoyancy due to the density variation initiated by the temperature difference,  $S_D$  represents the Darcy term which will be explained later how it is calculated.

#### 4. The enthalpy–porosity method

The enthalpy-porosity technique was used to deal with the issue of PCM melting. This methodology is predicated on the ratio between the volume of the PCM liquid and the overall volume of the PCM. The computational division of the storage unit domain will include categorizing it into three distinct zones: solid, liquid, and mushy. The partly solidified zone, the mushy region, is considered a porous medium in the enthalpy-porosity approach. Each cell's porosity (or liquid fraction) is assigned a number equivalent to its liquid component. In contrast, the porosity of the liquid zone is 1, while it varies between 0 and 1 for the mushy zone. The liquid fraction is computed as ([15], [16]):

$$f = \begin{cases} 0 & \text{if } T \leq T_s \\ \frac{T-T_s}{T_l-T_s} & \text{if } T_s \leq T \leq T_l \\ 1 & \text{if } T \geq T_l \end{cases} \quad (4)$$

where  $T_s$  and  $T_l$  are the solid and liquid phase transition temperatures of PCM.  $T$  refers to the temperature in this region.

The overall enthalpy  $H$  may be expressed as the summation of the sensitive enthalpy  $h$  and the latent enthalpy  $\Delta H$ , as explained by the equation. (3-5).

$$H = h + \Delta H \quad (5)$$

Where,

$$h = h_{ref} + \int_{T_{ref}}^T C_p dT \quad (6)$$

$$\Delta H = fL \quad (7)$$

$h_{ref}$  refers to the PCM sensible enthalpy at  $T_{ref}$ ,  $C_p$  to PCM specific heat at constant pressure, and  $L$  to the latent heat of PCM.

It is important to understand that the source term, also known as the Darcy term, denoted as  $S$  in the momentum equation (3-2). This is an essential method for dealing with the mushy zone.

$$S_D = \frac{(1-f)^2}{f^3+\varepsilon} V A_{mush} \quad (8)$$

In order to avoid a case of division by zero, a constant denoted as  $\varepsilon$  is used as a small number of 0.001. Also, the mushy zone constant  $A_{mush}$  is a continuous quantity that varies from  $10^4$  to  $10^7$  [17] and relates to the melting front's shape.

## 5. Initial and Boundary Conditions

The temperature of the inner tube's wall remains relatively constant, while the outer tube and the ends of the heat exchanger are thermally insulated. Furthermore, the heat transfer fluid (water) is pumped into the inner tube at different temperatures. As shown in Figure (1), The domain's boundary conditions are as follows:

**At time  $t=0$ , PCM and water temperatures =  $T_{ini} = 15^\circ\text{C}$**

**At time  $t > 0$**

$$U|_{r=r_i} = V = 0$$

$$T|_{r=r_i} = T_w = 70^\circ\text{C}$$

$$U|_{r=r_o} = V = 0$$

$$\frac{\partial T}{\partial r}\bigg|_{r=r_o} = 0$$

## 6. Computational model

The melting process of the phase change material (PCM) in an annular heat exchanger was simulated using ANSYS Fluent 17.2 software. The computational method is shown by a diagram, as presented in Fig. (2).

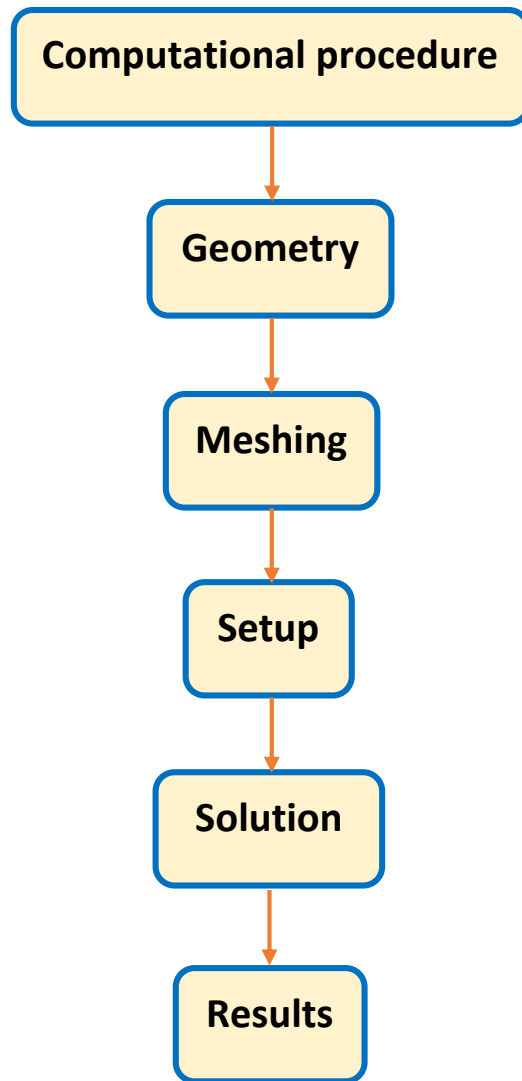


**Figure 2. Diagram for computational steps.**



## 7. The validation of the computational model

For the sake of the validity of the current model, it is necessary to conduct a comparative analysis with the experiment result or numerical findings acquired by different studies. This analysis should consider the similarity of the melting problem and the conditions of the study. The results obtained from the PCM melting process for the state without fins and an inner tube temperature of 70 °C were compared with the practical results obtained by Hussein et al. [6], which include melting RT50 as a PCM in a horizontal annular chamber with an inner tube diameter of 22 mm and an outer shell diameter of 85 mm. The water circulation in the inner tube at a temperature of 70°C leads to the melting of the PCM. Fig. (3) compares the numerical results of this study with the practical outcomes of Hussein et al. [6]. The utmost variance between the two outcomes is approximately 7%. The assumptions required to derive the numerical solution and experimental heat losses can both explain this variation.

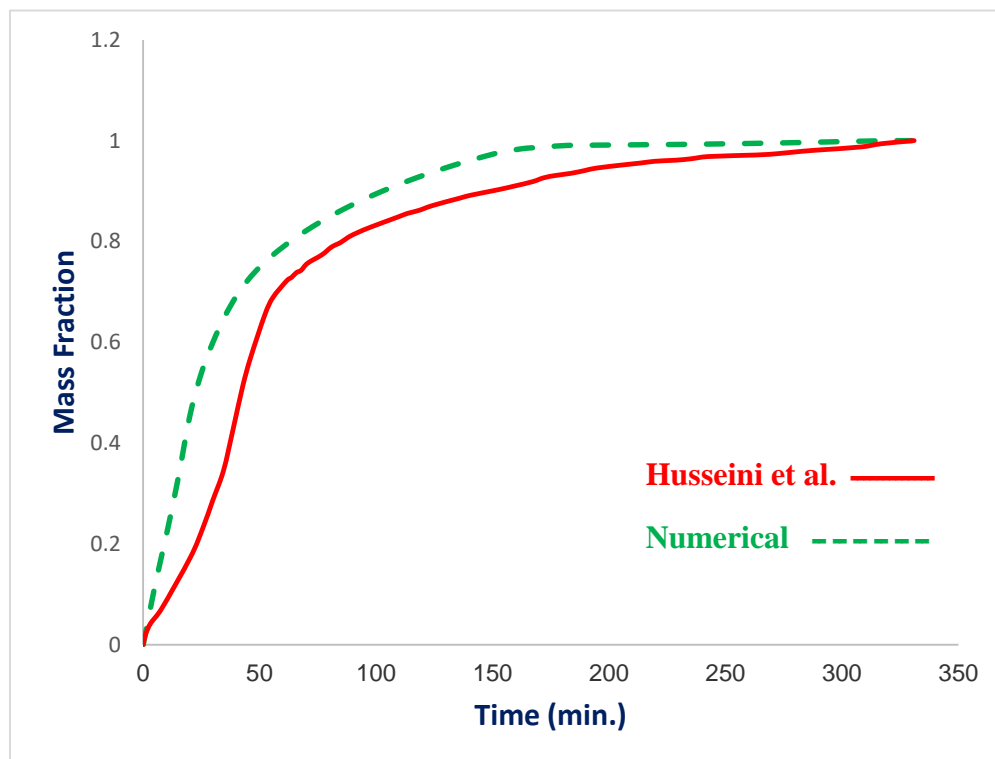


**Figure 3. Comparison between experimental result of Hussein et al. and present numerical results.**

## 8. Results

In this section, the numerical results for the effect of several factors on the melting of PCM and the progress of the melting interface will be discussed.

### 8.1 Mesh size- independence test

The mesh size independence test was conducted to find the most suitable number of mesh elements that achieve consistency between solution accuracy and the computational model's cost and implementation time. The investigation examines the impact of altering the molten material proportion on determining the most favorable mesh dimension. The PCM's starting temperature is recorded as 15 °C, while the water entering the system has an input temperature of 70 °C and a discharge rate of 6 l/min. Three groups of mesh size are examined: 2221, 5001, and 7653 elements. According to the investigation of a liquid fraction, the melting times of three different amounts of elements are 180, 182, and 185 minutes. Hence, the meshing technique 5001 is employed throughout the numerical investigation. The diagram shown in Fig. (4) explains the concept.

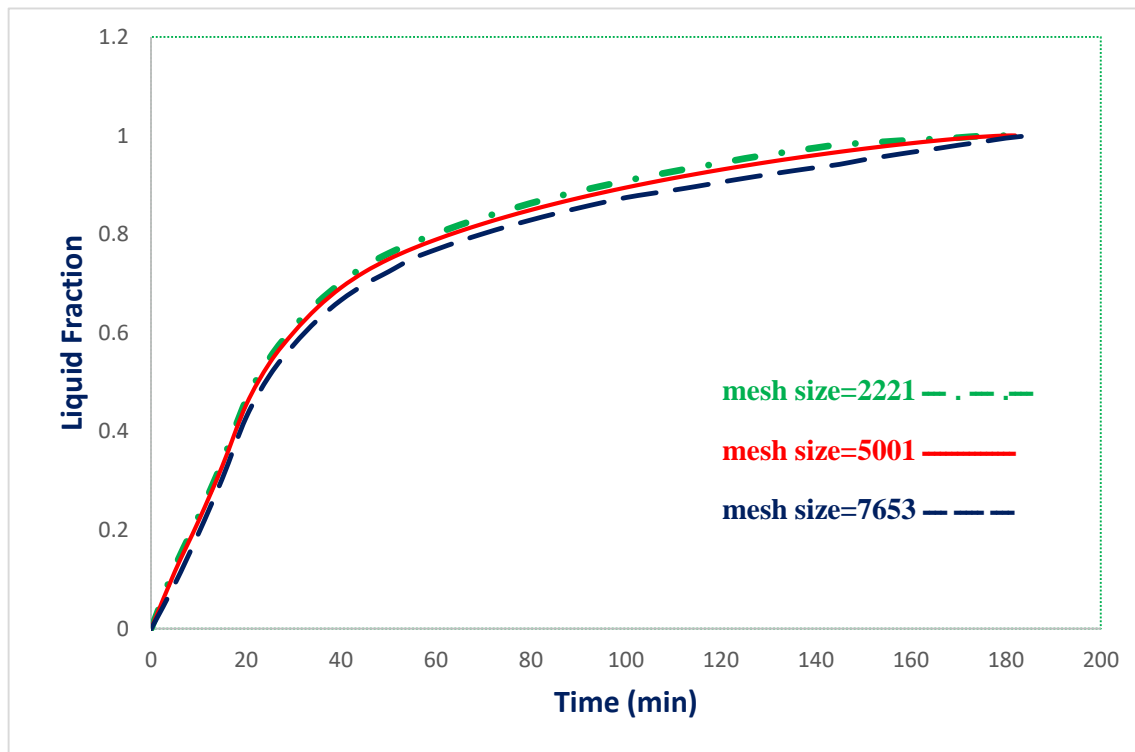
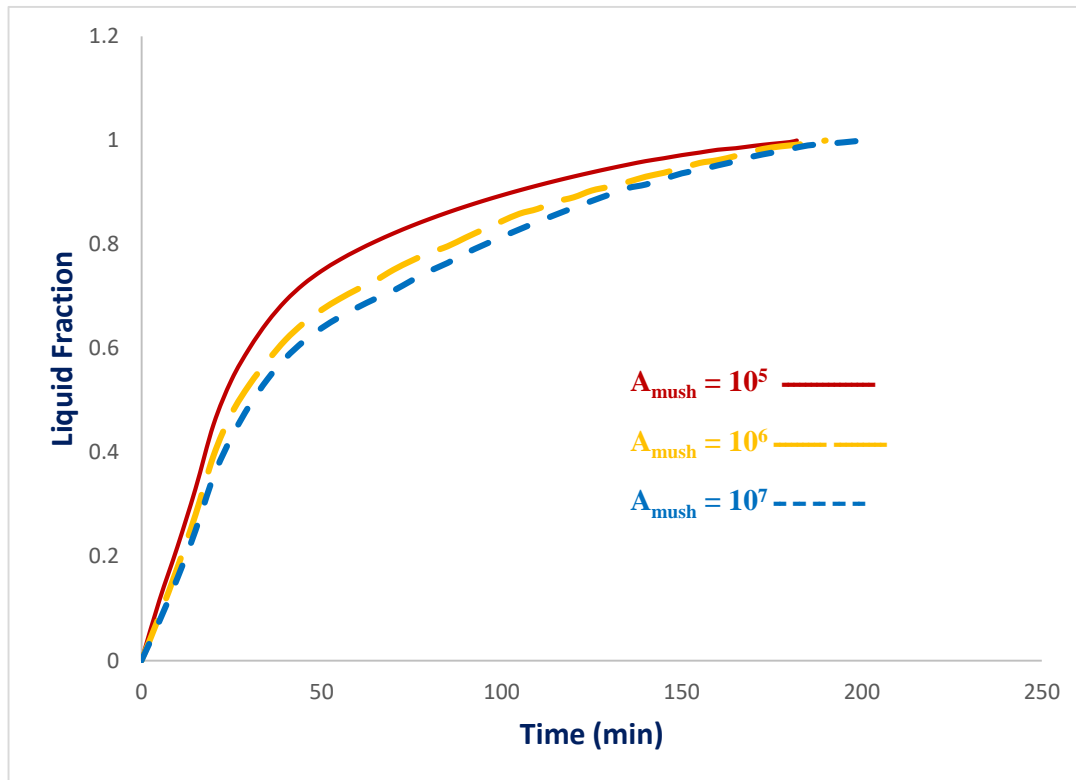


Figure 4. Test of mesh size-independence

### 8.2 The mushy zone constant independence test

Fig. (5) shows how the constants of the mushy zone affect the liquid fraction of PCM in the horizontal heat exchanger. The PCM's starting temperature is recorded as 15 °C, while the water entering the

system has an input temperature of 70 °C and a discharge rate of 6 l/min. Three mushy zone constants are examined:  $10^5$ ,  $10^6$ , and  $10^7$ .



**Figure 5. Independence test of the mushy zone.**

It is clear from the above diagram that melting time increases as constant values in the mushy zone rise. The melting times are 182, 191, and 200 minutes for mushy zone constants  $10^5$ ,  $10^6$ , and  $10^7$ , respectively.

### 8.3 The liquid fraction

The liquid (or melt) fraction represents the amount of melted PCM divided by the total amount of PCM. Fig. (6) explains the influence of the temperature of inlet HTF on the numerical values of the melt fraction of unfinned LHTES units.

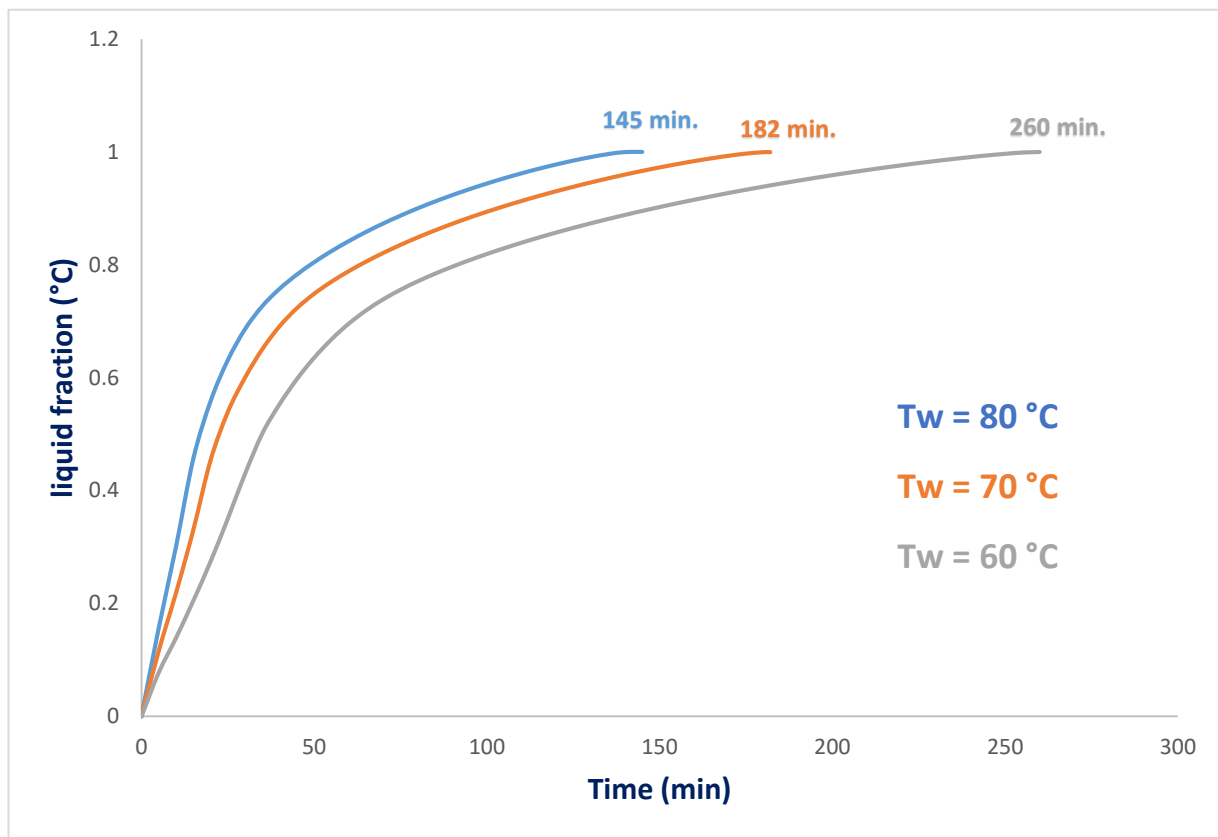


**Figure 6.** Effect of inlet HTF temperatures on the numerical liquid fractions for unfinned thermal storage unit.

It is shown that the water inlet temperature significantly affects the melting time. Therefore, by increasing the water inlet temperature, the amount of heat transferred from the source of the heat supply, the inner tube, to the PCM increases, leading to a reduction in the melting time. It can be noted that when using a water inlet temperature of 60 °C, the complete melting of PCM was 260 minutes. When using a water inlet temperature of 70 °C, the melting time decreased to 182 minutes, while the melting time reached 145 minutes when increasing the water inlet temperature to 80 °C.

#### 8.4 Progress of solid-liquid front

The transient progress of the solid-liquid interface is considered a significant feature of PCM melting. Fig. (7) shows an evolution of the melting front over time for three water inlet temperatures (60,70, and 80 °C).

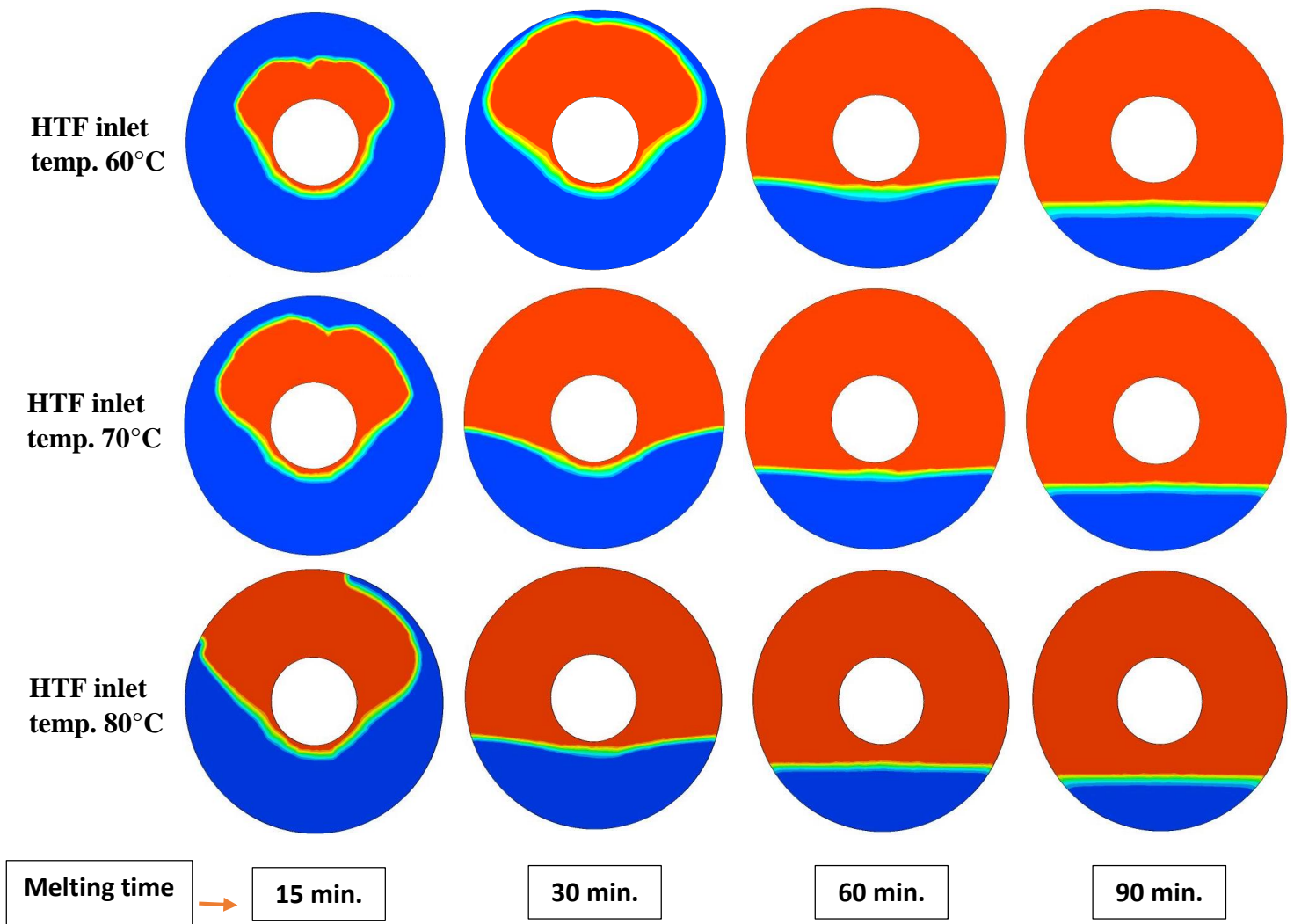


**Figure7.** Numerical progress of melting front

It is noted from the photographic illustration in Fig. (7) the effect of the water inlet temperature on the progress of the melting front.

### 8.5 Predicted temperature contours of PCM

The predicted results of the temperature contours for PCM inside a horizontal annular cavity heat exchanger are presented in Fig. (8) for the three different inlet water temperatures. The melting begins when the PCM temperature reaches the melting point. The molten PCM formed around the hot tub due to the predominant conduction heat transfer. Then, the buoyancy-driven convection has been developed, and PCM liquid ascends upward, leading to a higher melting rate at the upper part of the cavity. The melting rate at the bottom portion of the cavity takes longer than the upper part.

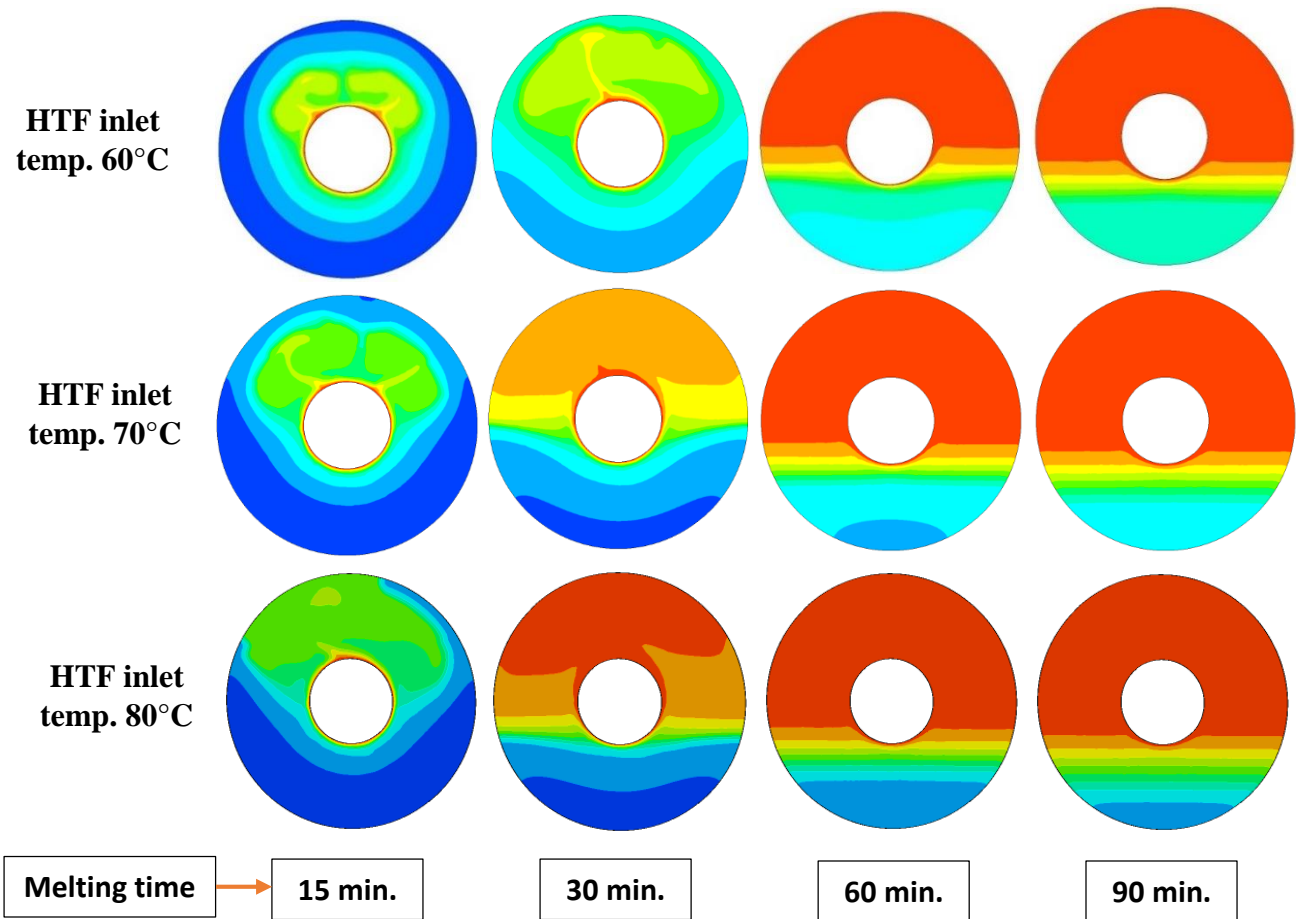


**Figure 8. temperature contours of PCM**

### 8.6 Streamlines of PCM melt

Fig. (9) presents the influence of HTF (water) inlet temperature on the melt velocity. The velocity of liquid PCM increases with increasing the temperature of the inlet water. Increasing the water temperature increases the transferred thermal energy into the PCM and excitation of rapid initiation of natural convection.

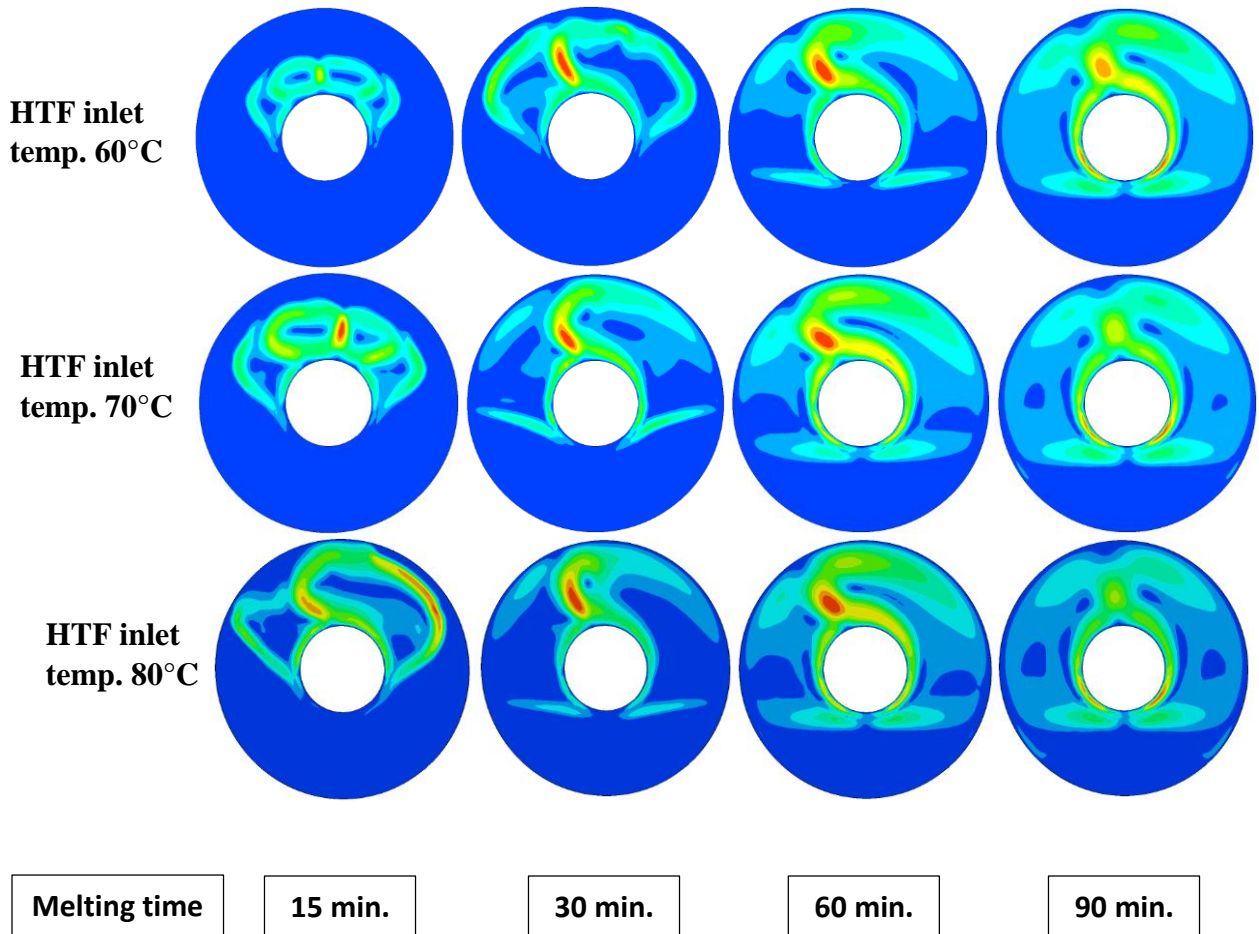


**Figure 9. Velocity contours of PCM.**

## 9. Conclusions

The numerical study of the melting process of PCM (RT-42 Rubitherm) in a horizontal (LHTES) unit was successfully investigated. Based on the parameters that were analyzed, it can be concluded the following:

1- At the beginning of the melting process, thermal conduction is dominant. Still, after forming a thin layer of liquid PCM near the inner tube, natural convection dominates, especially in the upper part of the heat exchanger.

- 2- HTF inlet temperature significantly affected the melting process of PCM. The melting of PCM was completed at 260, 182, and 145 minutes when water inlet temperatures of 60, 70, and 80 °C. That is, the melting time is reduced by 30% and 44% when using the water inlet temperature of 70 and 80 °C, respectively, relative to the water inlet temperature of 60 °C.
- 3- The best inlet temperature of HTF that gives the shortest melting time is 80 °C.
- 4- The melting time increases as mushy zone constant values rise, so the melting times are 182, 191, and 200 minutes for mushy zone constants  $10^5$ ,  $10^6$ , and  $10^7$ , respectively.
- 5- Depending on the above results, the constant for the mushy zone is appropriate set to  $10^5$ .
- 6- The meshing technique 5001 is employed throughout the whole of the numerical investigation.

## **References**

- [1] G. Chen and L. Wan, *Research and application of thermal storage with phase change materials*, vol. 250–253. 2011. doi: 10.4028/www.scientific.net/AMR.250-253.3541.
- [2] R. Dutta, A. Atta, and T. K. Dutta, “Experimental and Numerical Study of Heat Transfer in Horizontal Concentric Annulus Containing Phase Change Material,” vol. 86, no. August, pp. 700–710, 2008, doi: 10.1002/cjce.20075.
- [3] M. A. Ezan, M. Ozdogan, and A. Erek, “Experimental study on charging and discharging periods of water in a latent heat storage unit,” *Int. J. Therm. Sci.*, vol. 50, no. 11, pp. 2205–2219, 2011, doi: 10.1016/j.ijthermalsci.2011.06.010.
- [4] H. A. Adine and H. El Qarnia, “Numerical analysis of the thermal behaviour of a shell-and-tube heat storage unit using phase change materials,” *Appl. Math. Model.*, vol. 33, no. 4, pp. 2132–2144, 2009, doi: 10.1016/j.apm.2008.05.016.
- [5] A. R. Darzi, M. Farhadi, and K. Sedighi, “Numerical study of melting inside concentric and eccentric horizontal annulus,” *Appl. Math. Model.*, vol. 36, no. 9, pp. 4080–4086, 2012, doi: 10.1016/j.apm.2011.11.033.
- [6] M. J. Hosseini, A. A. Ranjbar, K. Sedighi, and M. Rahimi, “A combined experimental and computational study on the melting behavior of a medium temperature phase change storage



material inside shell and tube heat exchanger ☆,” *Int. Commun. Heat Mass Transf.*, vol. 39, no. 9, pp. 1416–1424, 2012, doi: 10.1016/j.icheatmasstransfer.2012.07.028.

- [7] M. Longeon, A. Soupart, J. Fourmigué, A. Bruch, and P. Marty, “Experimental and numerical study of annular PCM storage in the presence of natural convection,” *Appl. Energy*, vol. 112, pp. 175–184, 2013, doi: 10.1016/j.apenergy.2013.06.007.
- [8] W. Wang, K. Zhang, L. Wang, and Y. He, “Numerical study of the heat charging and discharging characteristics of a shell-and-tube phase change heat storage unit,” *Appl. Therm. Eng.*, vol. 58, no. 1–2, pp. 542–553, 2013, doi: 10.1016/j.applthermaleng.2013.04.063.
- [9] M. Avci and M. Y. Yazici, “Experimental study of thermal energy storage characteristics of a paraffin in a horizontal tube-in-shell storage unit,” *Energy Convers. Manag.*, vol. 73, pp. 271–277, 2013, doi: 10.1016/j.enconman.2013.04.030.
- [10] A. Agrawal and R. M. Sarviya, “Numerical investigation of the effects of natural convection on the melting process of phase change material in cylindrical annulus,” vol. 3, no. Iii, pp. 853–861, 2015.
- [11] A. K. Alshara, “Numerical Study for the Thermal Energy Storage Using PCM in Concentric Cylinders,” *Int. J. Appl. Comput. Math.*, vol. 4, no. 3, pp. 1–14, 2018, doi: 10.1007/s40819-018-0531-9.
- [12] W. A. Dukhan, N. S. Dhaidan, and T. A. Al-Hattab, “Experimental Investigation of the Horizontal Double Pipe Heat Exchanger Utilized Phase Change Material,” *IOP Conf. Ser. Mater. Sci. Eng.*, vol. 671, no. 1, 2020, doi: 10.1088/1757-899X/671/1/012148.
- [13] S. Seddegh, X. Wang, and A. D. Henderson, “A comparative study of thermal behaviour of a horizontal and vertical shell-and-tube energy storage using phase change materials,” *Appl. Therm. Eng.*, vol. 93, pp. 348–358, 2016, doi: 10.1016/j.applthermaleng.2015.09.107.
- [14] M. T. Jaffar Sathiq Ali, N. Manikandan, R. K. Jayaveeran, M. Asif Ahamed, and M. Alaguraj, “Experimental Evaluation of Shell & Tube Heat Exchanger With P-Toluidine (Pcm),” *Int. Res. J. Eng. Technol.*, pp. 2582–2586, 2019, [Online]. Available: [www.irjet.net](http://www.irjet.net)
- [15] S. Seddegh, M. Mastani, X. Wang, and F. Haghghat, “Experimental and numerical characterization of natural convection in a vertical shell-and-tube latent thermal energy storage

system,” *Sustain. Cities Soc.*, vol. 35, no. March, pp. 13–24, 2017, doi: 10.1016/j.scs.2017.07.024.

- [16] X. wen "Numerical and Experimental Study of the Melting Process of a Phase Change Material in a Partically Filled Spherical Shell" vol. 27, pp. 101306, 2017.Theses and Dissertations. 2888.
- [17] V.R. Voller, C. Prakash" A fixed grid numerical modelling methodology for convection-diffusion mushy region phase-change problems" vol. 27, pp. 1709-1719,1987 doi.org/10.1016/0017-9310(87)90317-6.
- [18] M. Akgu and K. Kaygusuz, “Experimental study on melting / solidification characteristics of a paraffin as PCM,” vol. 30, pp. 669–678, 2007, doi: 10.1016/j.enconman.2006.05.014.
- [19] H. Shmueli, G. Ziskind, and R. Letan, “International Journal of Heat and Mass Transfer Melting in a vertical cylindrical tube : Numerical investigation and comparison with experiments,” *Int. J. Heat Mass Transf.*, vol. 53, no. 19–20, pp. 4082–4091, 2010, doi: 10.1016/j.ijheatmasstransfer.2010.05.028.
- [20] Y. Wang, L. Wang, N. Xie, X. Lin, and H. Chen, “International Journal of Heat and Mass Transfer Experimental study on the melting and solidification behavior of erythritol in a vertical shell-and-tube latent heat thermal storage unit,” *HEAT MASS Transf.*, vol. 99, pp. 770–781, 2016, doi: 10.1016/j.ijheatmasstransfer.2016.03.125.
- [21] S. Ebadi, M. Al-Jethelah, S. H. Tasnim, and S. Mahmud, “An investigation of the melting process of RT-35 filled circular thermal energy storage system,” *Open Phys.*, vol. 16, no. 1, pp. 574–580, 2018, doi: 10.1515/phys-2018-0075.
- [22] M. Bechiri and K. Mansouri, “Study of heat and fluid flow during melting of PCM inside vertical cylindrical tube,” *Int. J. Therm. Sci.*, vol. 135, no. September 2018, pp. 235–246, 2019, doi: 10.1016/j.ijthermalsci.2018.09.017.
- [23] A. V. Waghmare and A. T. Pise, “Numerical Investigation of Concentric Cylinder Latent Heat Storage with / without Gravity and Buoyancy,” *Energy Procedia*, vol. 75, pp. 3133–3141, 2015, doi: 10.1016/j.egypro.2015.07.646.
- [24] S. Wang, Y. Guo, C. Peng, and W. Wang, “Experimental study of paraffin melting in cylindrical cavity with central electric heating rod,” *J. Environ. Manage.*, vol. 237, no. September 2018, pp. 264–271, 2019, doi: 10.1016/j.jenvman.2019.02.095.

- [25] I. Al Siyabi, S. Khanna, T. Mallick, and S. Sundaram, "Experimental and numerical study on the effect of multiple phase change materials thermal energy storage system," *J. Energy Storage*, vol. 36, no. December 2020, p. 102226, 2021, doi: 10.1016/j.est.2020.102226.
- [26] J. D. Chung, J. S. Lee, and H. Yoo, "Thermal instability during the melting process in an isothermally heated horizontal cylinder," *Int. J. Heat Mass Transf.*, vol. 40, no. 16, pp. 3899–3907, 1997, doi: 10.1016/S0017-9310(97)00037-9.
- [27] T. Kawanami, S. Fukusako, M. Yamada, and K. Itoh, "Experiments on melting of slush ice in a horizontal cylindrical capsule," *Int. J. Heat Mass Transf.*, vol. 42, no. 15, pp. 2981–2990, 1999, doi: 10.1016/S0017-9310(98)00340-8.
- [28] A. F. Regin, S. C. Solanki, and J. S. Saini, "Latent heat thermal energy storage using cylindrical capsule: Numerical and experimental investigations," *Renew. Energy*, vol. 31, no. 13, pp. 2025–2041, 2006, doi: 10.1016/j.renene.2005.10.011.
- [29] M. Hlimi *et al.*, "Melting inside a horizontal cylindrical capsule," *Case Stud. Therm. Eng.*, vol. 8, no. September, pp. 359–369, 2016, doi: 10.1016/j.csite.2016.10.001.
- [30] P. R. Ansyah, J. Waluyo, Suhanan, M. Najib, and F. Anggara, "Thermal behavior of melting paraffin wax process in cylindrical capsule by experimental study," *AIP Conf. Proc.*, vol. 2001, 2018, doi: 10.1063/1.5049968.

#### دراسة حسابية لشحن المواد متغيرة الطور في نظام تخزين الطاقة الحرارية الكامنة

**الخلاصة:** يقدم هذا البحث تحقيقاً حسابياً لخصائص شحن مواد متغيرة الطور داخل وحدة تخزين الطاقة الحرارية الكامنة التي تتكون من مبادل حراري أفقي من نوع الأنبوب الداخلي والغلاف الخارجي باستخدام برنامج (ANSYS/FLUENT). تم اختبار عملية الذوبان عددياً لدرجة حرارة مدخل سائل نقل الحرارة (الماء) (60 و 70 و 80 درجة مئوية)، ودرجة الحرارة الأولية لمواد متغيرة الطور هي 15 درجة مئوية. كما تناولت هذه الدراسة تأثير ثابت المنطقة الطرية على عملية الذوبان. تظهر النتائج الشاملة أن وقت الشحن يتناقص مع زيادة درجة حرارة مدخل الماء ويكتمل ذوبان المادة متغيرة الطور في زمن قدره 260 دقيقة عند استخدام درجة حرارة مدخل الماء 60 درجة مئوية، بينما يصل وقت الذوبان إلى 182 دقيقة عندما تكون درجة حرارة مدخل الماء 70 درجة مئوية، ويكتمل الذوبان في زمن قدره 145 دقيقة باستخدام درجة حرارة دخول الماء الساخن 80 درجة مئوية. عند زيادة درجة حرارة مدخل الماء من 60 إلى 70 و 80 درجة مئوية على التوالي، يتم تخفيض وقت الذوبان بحوالي 30% و 44%. أفضل تخفيض لوقت الانصهار تم الحصول عليه عند استخدام درجة حرارة مدخل الماء 80 درجة مئوية. بالإضافة إلى ذلك يبين النتائج أن وقت الذوبان ازداد مع ارتفاع قيم ثابت المنطقة الطرية المستخدمة. حيث كانت أوقات الذوبان 182، 191، و 200 دقيقة لثوابت المنطقة الطرية  $10^5$ ،  $10^6$ ، و  $10^7$  على التوالي. لذلك فإن استخدام ثابت المنطقة الطرية البالغ  $10^5$  يعطي أفضل تخفيض في وقت الذوبان.

**الكلمات المفتاحية:** مواد متغيرة الطور، شحن، الحمل الطبيعي، وقت الذوبان.